arXiv:1703.08173v1 [cs.CV] 23 Mar 2017

Single Image Super-resolution with a Parameter Economic Residual-like Convolutional Neural Network

$YudongLiang^1$, $ZeYang^1$, $KaiZhang^2$, $YihuiHe^1$, $JinjunWang^1$, and $NanningZheng^1$

[1]Institute of Artificial Intelligence and Robotics, Xi'an Jiaotong University, Xi'an, Shaanxi, China, 710049
[2] Harbin Institute of Technology, China

Abstract. *Recent years have witnessed great success of convolutional neural network (CNN) for various problems both in low and high level visions. Especially noteworthy is the residual network which was originally proposed to handle high-level vision problems and enjoys several merits. This paper aims to extend the merits of residual network, such as skip connection induced fast training, for a typical low-level vision problem, i.e., single image super-resolution. In general, the two main challenges of existing deep CNN for supper-resolution lie in the gradient exploding/vanishing problem and large amount of parameters or computational cost as CNN goes deeper. Correspondingly, the skip connections or identity mapping shortcuts are utilized to avoid gradient exploding/vanishing problem. To tackle with the second problem, a parameter economic CNN architecture which has carefully designed width, depth and skip connections was proposed. Different residual-like architectures for image superresolution has also been compared. Experimental results have demonstrated that the proposed CNN model can not only achieve state-of-the-art PSNR and SSIM results for single image super-resolution but also produce visually pleasant results. This paper has extended the mmm 2017 paper with more experiments and explanations.*

Keywords: super-resolution, deep residual-like convolutional neural network, skip connections, the mount of parameters

1 Introduction

Single image super-resolution (SISR) which aims to recover a high-resolution (HR) image from the corresponding low-resolution (LR) image is a practical technique [22,21,11] due to its high value in various fields. Typically, it is very challenging to restore the missing pixels from an LR observation since the number of pixels to be estimated in the HR image is usually much larger than that in the given LR input. Generally, SISR techniques can be roughly divided into three categories: the interpolation methods, the reconstruction methods [8] and the example based methods [4,20].

Most of the recent SISR methods fall into the example based methods which try to learn prior knowledge from LR and HR pairs, thus alleviating the ill-posedness of SISR. Representative methods include neighbor embedding regression [1,16,17], random forest [14,13] and deep convolutional neural network (CNN) [2,3,12,9].

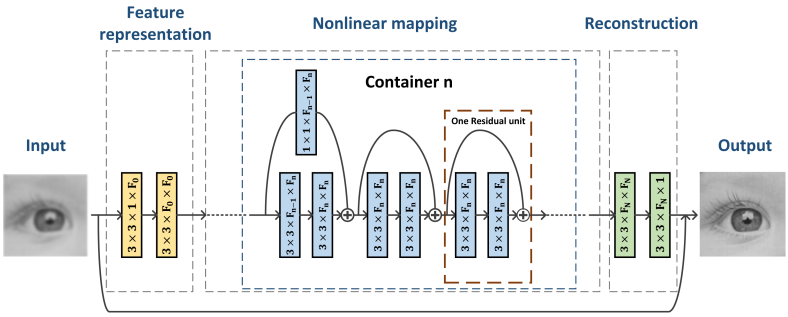

Fig. 1. The architecture of our residual-like model.

Among the above techniques, deep learning techniques especially deep CNN have largely promoted the state-of-the-art performances in SISR area. Dong *et al.* [2] proposed a deep convolutional neural network termed SRCNN with three convolutional layers for image super-resolution. By learning an end-to-end mappings from LR to HR images, SRCNN extracts more discriminative features than handcrafted ones. Later, Dong *et al.* [3] extended SRCNN with larger filter size and filter numbers while keeping the depth of CNN fixed to further improve the performance. They have found that deeper model was hard to train and they failed to boost the performance by increasing the depth. Such findings indicate that deeper model is not suitable for image super-resolution, which is counter-intuitive as deeper model have been proved more effective in many tasks [15,5,6]. Instead of directly predicting the HR output, Kim *et al.* [9] proposed a very deep CNN (VDSR) with depth up to 20 to predict the residual image. VDSR surpasses SRCNN with a large margin which mainly benefits from two aspects: deeper architecture and predicting high frequency of images only which is called residual learning by [9].

As demonstrated in [9], the SR results have been improved as VDSR goes deeper. Although VDSR has achieved impressive results, the plain structure of VDSR which simply stacks layers hampers the convergence of deeper architectures due to the gradient exploding/vanishing problem. It would not bring any improvement as the network goes deeper. Fortunately, the residual network [5,6] has successfully addressed this issue. As a result, different from VDSR, this paper has designed a novel very deep residual-like convolutional neural network whose architecture is shown in Fig. 1. As LR image and target HR image is highly correlated, predicting high frequency of the image only is a kind of residual

learning which largely lower the price for training. Thus, a totally residual-like deep CNN will fully take advantage of the correlations between LR and HR images. Moreover, skip connections or identity mapping shortcuts in residual-like deep CNN would alleviate gradient vanishing/exploding problem when the network becomes increasingly deeper.

While very deep CNN model would increase the model capacity, on the other hand, it would introduce a huge amount of parameters which is sometimes unacceptable for limited hardware. Thus, a computational economic architecture is essential for real word applications. In this paper, the 'shape' of deep CNN has been explored to largely reduce the amount of parameters. The 'shape' of deep CNN refers to all the filter size and numbers of each layer which decides featuremap size and numbers of each layer to form a global shapes. With a residual-like architecture and economic shape design, the proposed model can not only achieve state-of-the-art PSNR and SSIM results for single image super-resolution but also produce visually pleasant results.

2 Related Works

In the pioneer work by Freeman *et al.* [4], the co-occurrence priors were proposed that similar LR local structures often relate to similar HR local information. From LR and corresponding HR images, LR and HR examples (patches or sub images) could be extracted to form training database. The mappings from LR to HR examples call for accurate regression methods to be applied.

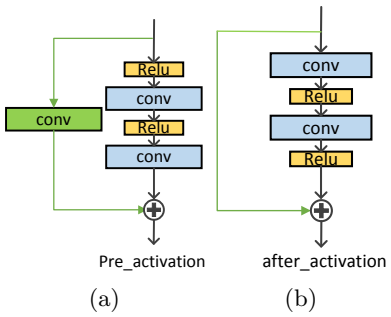

Fig. 2. Different architecture cells of CNN

Since the work of SRCNN[2], deep CNNs have refreshed the state-of-the-art performances in super-resolution area. Dong *et al.* [3] elaborated the filter size and filter numbers for their three layers of SRCNN which further improved the performance. Wang *et al.* [18] incorporated the sparse coding prior into CNN architecture design based on the learned iterative shrinkage and thresholding algorithm (LISTA). With sparsity prior modeling, the performance boosted even with a model of smaller size compared with SRCNN.

Currently, the best performance and deepest CNN architecture for image super-resolution was VDSR with 20 convolutional layers proposed by Kim et al [9], which largely accelerated the speed of training and outperformed SRCNN presented by Dong et al[3]. To ensure the fast convergence of deep CNN and avoid gradient vanishing or exploding, a much larger learning rate for training was cooperated with adjustable gradient clipping in VDSR training. VDSR is inspired by the merits of VGG net which attempts to train a thin deep network. However, this kind of plain networks are not easy to be optimized when it goes even deeper as demonstrated by He *et al.* [5,6].

The difficulties of training deeper plain networks were carefully analyzed by He *et al.* [5,6]. It has been observed that the testing accuracy even the training accuracy becomes saturated then degrades rapidly as plain networks goes deeper, which is called as the degradation problem [5]. This degradation is caused by the difficulties of training other than overfitting. It has been demonstrated that learning a residual function is much more easier than learning the original prediction function with very deep CNN. Residual networks with a surprising depth were designed for image classification problems with skip connections or identity mapping shortcuts. Later, a detailed analysis on the mechanisms of identity mapping in deep residual networks and a new residual unit design has been represented in [6].

After largely easing the difficulties of training much deeper CNN with residual functions by shortcuts or skip connections, the huge amount of parameters is still a big problem for computational resources and storage. He *et al.* [5,6] attempts to alleviate the problem by bottleneck architectures. The bottleneck architectures first utilized 1×1 convolutions to reduce the dimensions, then after some operations, 1×1 convolutions are applied again to increase the dimensions. With such a residual unit design, the amount of parameters was largely reduced. Thus, the shape of CNN could be potentially explored to reduce the parameters while maintain the performances. In the meanwhile, contextual information is very important for image super-resolution, such residual unit design may give a negative effort to the SR results.

With a carefully design and exploration of the shape of the network, a novel residual-like deep model is proposed for image super-resolution task.

3 A Parameter Economic Residual-like Deep Model for Image Super-resolution

Following the example based methods, HR examples I^h and LR examples I^l are extracted from HR images I^H and LR images I^L respectively. The degeneration process of LR images I^L from the corresponding HR images I^H could be considered as the following blurring process related with blur kernel G and downsampling process $\downarrow_s$ with a a scale factor s as in Eq.(1).

$$I^L = (I^H \otimes G) \downarrow_s, \tag{1}$$

3.1 Residual-like Deep Model

Our residual-like deep CNN for image super-resolution is an end-to-end mapping model which tries to predict HR versions from LR input ones. There are three sub-networks in our deep CNN to perform three steps: feature representation, nonlinear mapping, reconstruction.

The feature representation sub-network extracts discriminative features from the LR input images, while nonlinear mapping part maps the LR feature representations into HR feature representations. Reconstruction part restores the HR images from HR feature representation. Feature representation apply plain network stacking convolutional and ReLU layers as shown in Fig. 1 and reconstruction use convolutional layers. The main body of our model, nonlinear mapping part consists of residual-like units which eases the difficulties of training.

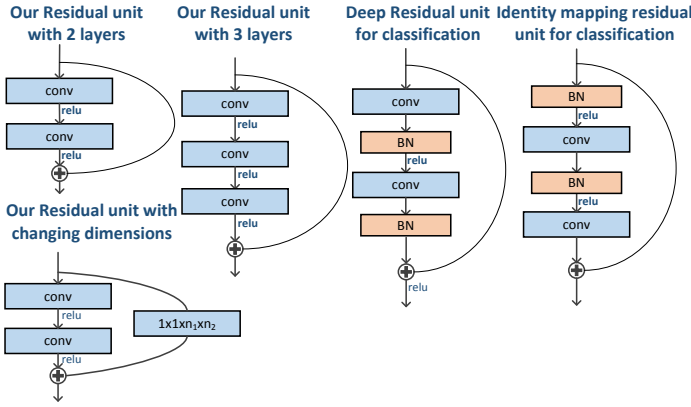

Fig. 3. The architectures of different residual units.

Typical units of our residual-like deep CNN are shown in Fig. 3. As residual unit with 2 layers and 3 layers worked well for image super-resolution problem, those two kinds of units are applied in the experiments. When featuremap dimensions change, the identity shortcut becomes a projection to change feature dimensions. The second right and rightmost are one unit of residual net for image classification problems proposed by He *et al.* in [5,6] respectively. The architectures of our residual functions are composed of convolutional, ReLU layers and shortcuts, which is very different. Batch normalization units are discarded and deployments are different. Similar with VDSR, small convolutional filter size as 3×3 has been applied. Shortcuts or skip connections which are identity mappings are realized by element-wise additions. As this element-wise addition increases very little computations, our feed-forward deep CNN has a similar computational complexity with VDSR. Assuming the input as x^k of kth residual unit, the residual functions have the following form:

$$x^{k+1} = x^k + f(\theta^k, x^k), \tag{2}$$

where θ^k are the parameters of kth residual unit. As predicting high frequency can boost the performances and convergence speeds of deep CNN [9], a simple Euclidean loss function is adopted to approximate the high frequencies of examples

$$loss = \frac{1}{2n}\sum_{i=1}^{n} \|F(\Theta, I_i^l) - (I_i^h - I_i^l)\|^2 \tag{3}$$

where n is the number of patch pairs (I^l, I^h), $F(\Theta, I^l)$ denotes the predictions of our residual-like deep CNN with parameter Θ. Our residual-like deep CNN is composed of several **Container**s which have certain number of residual units. For succinctness, the filter numbers keep the same in each single container. The architectures of our residual-like deep CNN will be described as a sequence of the filter numbers ($N1_{k1}$, $N2_k$, $\cdots$) in containers. If subscript k exists for N_k, it means there are k residual units with each having a filter number of N.

Stochastic gradient descent (SGD) with the standard back-propagation [10] is applied to train our residual-like deep CNN. In particular, the parameter is updated as Eq. (4), where m denotes the momentum parameter with a value of 0.9 and η is the learning rate.

$$\triangle_{i+1} = m \cdot \triangle_i + \eta \cdot \frac{\partial loss}{\partial \theta_i}, \quad \theta_{i+1} = \theta_i + \triangle_{i+1} \tag{4}$$

High learning rates are expected to boost training with faster and better convergency. Adjustable gradient clipping [9] is utilized to keep learning rates high while at the same time to prevent the net from gradient exploding problems. Gradients $\frac{\partial Loss}{\partial \theta_i}$ are clipped into the range of $[-\frac{\tau}{\eta}, \frac{\tau}{\eta}]$, where τ is a constant value.

3.2 Economic Design for the Proposed Model

In this paper, the 'shape' of deep CNN has been explored to reduce the amount of parameters. The 'shape' of deep CNN is determined by all the filter size and numbers of each layer. Thin but small filter size works well with padding which leads to larger receptive field as network goes deep, in specific, 3×3 filter size has been applied. Next, filter numbers and the combinations of filter numbers will be discussed.

Exploring the Shape of the Architecture Inspired by the bottle-neck architecture [6], this paper supposes that changing the shape of the architecture may maintain the performance while largely reduces the computational parameters. Instead of applying 1×1 convolutions as bottle-neck architecture, the 3×3 convolutions are applied as image SR process largely depends on the contextual information in local neighbor areas. The impacts of the featuremaps number in each layers on performance are carefully explored in the following fashions: increase monotonically, decrease monotonically, increase monotonically then decrease monotonically, decrease monotonically then increase monotonically. The experiments demonstrate that some of different economic designs have achieved

comparable performance which largely reduce the parameters. This will be further discussed in the experiments part. In comparison with our residual-like CNN, the performances of VDSR with different shapes have more variations. This proves our residual-like architecture are more robust to the shape of CNN.

Training with Multiple Upscaling Factors It has been pointed out that it is feasible to train a deep CNN for different upscaling factors [9]. Training datasets for different specified upscaling factors are combined together to enable our residual-like deep CNN to handle multiple upscaling factors, as images across different scales share some common structures and textures. Parameters are shared across different predefined upscaling factors which further dispense with the trouble of retaining different models for different upscaling factors.

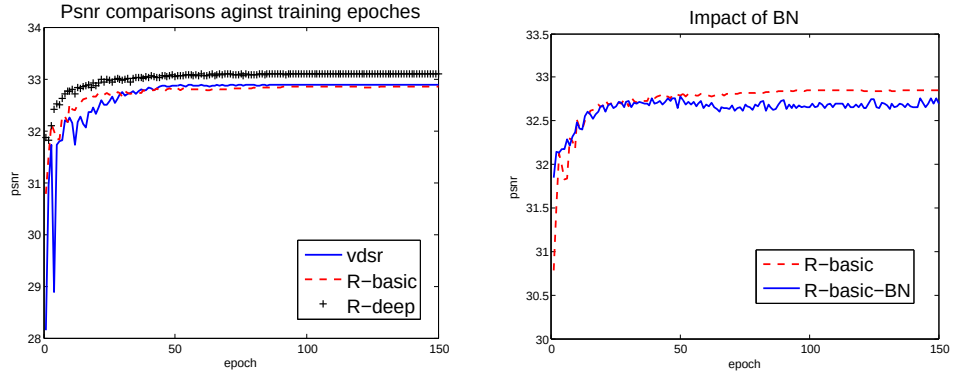

(a)Comparison among R-deep, R-basic and VDSR (b) The impacts of BN

Fig. 4. Comparison of test psnr of Set 14 against training epoch among (a) R-deep, R-basic and VDSR, (b)our R-basic with and without Batch Normalization(BN).

4 Experiments

In this section, we conducted a series of experiments to demonstrate the performance of the proposed method against the state-of-the-art SISR methods.

The same 291 training images applied by VDSR were utilized for training, including 91 images proposed in Yang *et al.* [20] and 200 natural images from Berkeley Segmentation Dataset (BSD). For testing, four datasets were investigated: 'Set5' and 'Set14' [16,2],'Urban100' [7] and 'BSD100' [16,19].

The size of example is set as 41×41 and the batch size is set as 64. Momentum and weight decay parameters are fixed as 0.9 and 0.0001 respectively. Multi-scale training is applied in all of the following experiments. Weight initialization methods [5,6] were applied. Learning rate was initially set to 0.1 and then

decreased by a factor of 10 every 30 epochs. All these setting ensures us to make a fair comparison with the competing approaches including VDSR method.

4.1 Comparisons with the State-of-the-art Methods

Table 1 shows the quantitative comparisons with A+ [17], RFL [14], SelfEx [7], SRCNN [2] and VDSR [9]. Visual results were also demonstrated to give intuitive assessment. In table 1, two architectures of our residual-like deep CNN with different depth have been investigated, denoted as **R-basic** and **R-deep** respectively. R-basic $(16_3, 32_3, 64_3)$ has 22 layers, while R-deep $(16_3, 32_3, 64_3, 128_3, 256_3)$ has 34 layers. Deeper and larger model R-deep has achieved the best performance compared with other methods in most cases and comparable results in other situation.

R-basic outperform the other methods except VDSR. However, the performances of VDSR (20 layers) have not been obtained by us. For example, the average PSNR of VDSR for Set5 and Set14 are 37.32dB and 32.89dB respectively. Assisted with the missing tricks, the performance of our model is expected to be further boosted. In Fig. 4, the PSNR against training epochs has been compared among R-basic, R-deep, and VDSR trained by us. Deeper and larger model R-deep outperformed VDSR at very beginning with a large margin. Although R-basic contained much less parameters, R-basic model has obtained comparable performances with VDSR.

In Fig. 5, all the compared results are obtained by the released code of the authors. Visual pleasing restorations have been achieved by our model. Results of our method contain more authentic texture and more clear details compared with other methods such as the texture of the zebra head. Our method have provided less artifacts, *e.g.* all the other methods except ours have restored obvious artifacts at the location of book. Shaper edges have appeared in our restorations which have represented visually more pleasing results.

Table 1. Comparison in different datasets and with different scales.

Dataset	Scale	Bicubic PSNR/SSIM	A+[17] PSNR/SSIM	RFL[14] PSNR/SSIM	SelfEx[7] PSNR/SSIM	SRCNN[2] PSNR/SSIM	VDSR[9] PSNR/SSIM	R-deep PSNR/SSIM	R-basic PSNR/SSIM
Set5	×2	33.66/0.9299	36.54/0.9544	36.54/0.9537	36.49/0.9537	36.66/0.9542	**37.53/0.9587**	37.51/**0.9587**	37.27/0.9577
	×3	30.39/0.8682	32.58/0.9088	32.43/0.9057	32.58/0.9093	32.75/0.9090	33.66/0.9213	**33.72/0.9215**	33.43/0.9190
	×4	28.42/0.8104	30.28/0.8603	30.14/0.8548	30.31/0.8619	30.48/0.8628	31.35/**0.8838**	**31.37/0.8838**	31.15/0.8796
Set14	×2	30.24/0.8688	32.28/0.9056	32.26/0.9040	32.22/0.9034	32.42/0.9063	33.03/0.9124	**33.10/0.9131**	32.86/0.9113
	×3	27.55/0.7742	29.13/0.8188	29.05/0.8164	29.16/0.8196	29.28/0.8209	29.77/0.8314	**29.80/0.8317**	29.67/0.8297
	×4	26.00/0.7027	27.32/0.7491	27.24/0.7451	27.40/0.7518	27.49/0.7503	28.01/0.7674	**28.06/0.7681**	27.90/0.7648
BSD100	×2	29.56/0.8431	31.21/0.8863	31.16/0.8840	31.18/0.8855	31.36/0.8879	31.90/0.8960	**31.91/0.8961**	31.76/0.8940
	×3	27.21/0.7385	28.29/0.7835	28.22/0.7806	28.29/0.7840	28.41/0.7863	28.82/0.7976	**28.83/0.7980**	28.73/0.7954
	×4	25.96/0.6675	26.82/0.7087	26.75/0.7054	26.84/0.7106	26.90/0.7101	**27.29/0.7251**	27.27/0.7248	27.19/0.7221
Urban100	×2	26.88/0.8403	29.20/0.8938	29.11/0.8904	29.54/0.8967	29.50/0.8946	30.76/0.9140	**30.88/0.9150**	30.47/0.9100
	×3	24.46/0.7349	26.03/0.7973	25.86/0.7900	26.44/0.8088	26.24/0.7989	27.14/0.8279	**27.17/0.8283**	26.92/0.8208
	×4	23.14/0.6577	24.32/0.7183	24.19/0.7096	24.79/0.7374	24.52/0.7221	25.18/0.7524	**25.22/0.7537**	25.02/0.7452

Impacts of Batch Normalization on SISR It seems adding batch normalization (BN) operations has hampered further improvement when more epoches have been performed. Normalizing input distribution of mini-batch to suppress

data shifting has been proved powerful and largely accelerated the training convergency speed. It also enable deeper architecture and larger learning rates to be utilized in other tasks. However, whiten input and output of the intermediate layer may not be suitable for image super-resolution task which need precise output. Another suspects may be regularization effects of BN has not been fully exploited as the training set of Fig. 4(b) is still limited in contrast with ImageNet. As larger learning rates were enabled by gradient clipping methods, the benefits of BN for leaning rates are alleviated. The experiments with impacts of BN on SR would be elaborated in the future.

4.2 Amount of Parameters

For R-basic model, there are 22 convolutional layers and 0.3M(322721) parameters accumulated by the amounts of corresponding weights and bias. For R-deep model, 34 convolutional layers and 5M(4975905) parameters are applied. The compared VDSR in Table 1 is 20 layers and has 0.7M(664704) parameters. Although R-deep has more parameters, our R-deep model is still acceptable which can be efficiently trained with single GPU.

4.3 The Deeper the Better, the Wider the Better

R-deep model perform much better than R-basic. Next, ablations of our system would be evaluated to unpack this performance gain. Two factors, width which is relate to filter numbers and depth of our model would be analyzed.

First, 20 layer VDSR has been added with identity shortcuts to form a residual-like net, $R(64_8)$. The performance of $R(64_8)$ is roughly the same as VDSR in Table 2. The shortcuts have very little impacts on the descriptive power.

Table 2. PSNR comparison between our residual-like CNN and VDSR trained by us

	Set5	Set14	BSD100	Urban100
$R(64_8)$	37.28	32.91	31.72	30.45
VDSR	37.32	32.89	31.77	30.51

Second, fixed the depth of model, simply broadened the width will improve the performance, *e.g.* , $R(16_3, 32_3, 64_3)$ vs $R(32_3, 64_3, 128_3)$, $R(4_3, 8_3, 16_3, 32_3, 64_3)$ vs $R(16_3, 32_3, 64_3, 128_3, 256_3)$

Third, the deeper the architecture, the better the performance. Adding one more residual unit, *e.g.* , $R(16, 32, 64, 128)$ vs $R(32, 64, 128)$ will improve the performance. Certainly, the depth should be no more than certain number to avoid the overfitting problem as the training data is limited. Within this limit, the deeper the better. Our residual-like unit eases the training difficulties which enables a deeper CNN architecture to improve the situation. On the other side,

plain deep CNN VDSR with a same depth as our residual-like R-deep model can not converge well and the restorations deteriorate. Another attempt to facilitate deeper net which is the economic design to solve the problem of parameter amounts will be discussed next.

Table 3. PSNR by the residual-like model of different depths and width with a magnification factors 2 in Set14.

	$R(16_3, 32_3, 64_3)$	$R(32_3, 64_3, 128_3)$	$R(16_3, 32_3, 64_3, 128_3)$	$R(16_3, 32_3, 64_3, 128_3, 256_3)$	$R(4_3, 8_3, 16_3, 32_3, 64_3)$
PSNR(dB)	32.85	32.96	33.00	33.10	32.91

4.4 Economic Design

The performances of different architectures which have different shapes have been investigated for our residual-like net and VDSR counterpart. To be specific, there are 28 layers as 6 residual **container**s stack and each **container** contains 2 residual units (2 layers). It can be calculated as $28 = 2 + 6 \times 2 \times 2 + 2$, where feature representation sub-network and reconstruction sub-network each have 2 layers. For VDSR, 12 layers VDSR have been explored. For residual-like architecture, different architectures have achieved comparable results. Analysis about the reasons and more detailed experiments will be investigated in the future.

Table 4. Performance by different residual-like models which have different shapes with a magnification factor 2 in Set14.

residual	$R(16_4, 32_4, 64_4)$	$R(64_4, 32_4, 16_4)$	$R(16_2, 32_2, 64_2, 64_2, 32_2, 16_2)$	$R(64_2, 32_2, 16_2, 16_2, 32_2, 64_2)$
PSNR(dB)	32.91	32.85	32.94	32.89

Table 5. Performance by VDSR which have different shapes with a magnification factor 2 in Set14.

VDSR	$(8_2, 16_2, 64_2)$	$(64_2, 16_2, 8_2)$	$(8, 16, 64, 64, 16, 8)$	$(64, 16, 8, 8, 16, 64)$	(64_{16})
PSNR(dB)	32.68	32.59	32.66	32.50	32.85

5 The Position of RelU

Then performance compared with the positions of ReLU layers (ReLU before/after conv) as Fig 2 respectively are represented in Table 6 for Set14. Convolutional layers of the same depth among these networks have the same parameters.

From the results in Table 6, we conclude that the position of Relu make small differences.

Table 6. Ablation comparisons of convolutional skip vs identity skip connections, the order of convolution and ReLU layers in terms of average PSNR (dB) on Set14.

scale	identity+ after_act	identity+ pre_act
×2	32.97	33.01
×3	29.75	29.77
×4	28.02	28.02

6 Training with Multiple Upscaling Factors vs Single Scale

In this section, we compare the performances of network trained by different training Samples, multiple upscaling factors vs single scale in Table 7.

Table 7. PSNR comparison between our residual-like CNN and VDSR trained by us

		Set5	Set14	BSD100	Urban100
		PSNR/SSIM	PSNR/SSIM	PSNR/SSIM	PSNR/SSIM
$\otimes 2$	Multiscale	37.51/0.9587	**33.10/0.9131**	**31.91/0.8961**	**30.88/0.9150**
	single scale	**37.52/0.9589**	33.03/0.9129	31.90/0.8958	30.84/0.9143
$\otimes 3$	Multiscale	**33.72/0.9215**	**29.80/0.8317**	**28.83/0.7980**	**27.17/0.8283**
	single scale	33.6/0.9212	29.75/0.8313	28.79/0.7967	27.08/0.8255
$\otimes 4$	Multiscale	**31.37/0.8838**	**28.06/0.7681**	**27.29/0.7251**	**25.22/0.7537**
	single scale	31.30/0.8824	27.99/0.7668	27.24/0.7237	25.14/0.7051

It seems mixing samples from different upscaling factors has slightly boosted the performances, especially for large upscaling factors.

7 conclusion

In this paper, a novel residual-like deep CNN which takes advantage of skip connections or identity mapping shortcuts in avoiding gradient exploding/vanishing problem was proposed for single image super-resolution. In particular, the shape of CNN has been carefully designed such that a very deep convolutional neural network with much fewer parameters can produce even better performance. Experimental results have demonstrated that the proposed method can not only achieve state-of-the-art PSNR and SSIM results for single image super-resolution but also produce visually pleasant results.

Acknowledgments. This work is partially supported by National Science Foundation of China under Grant NO. 61473219.

References

1. Chang, H., Yeung, D.Y., Xiong, Y.: Super-resolution through neighbor embedding. In: Computer Vision and Pattern Recognition, 2004. CVPR 2004. Proceedings of the 2004 IEEE Computer Society Conference on. vol. 1, pp. I–275. IEEE (2004) 2
2. Dong, C., Loy, C.C., He, K., Tang, X.: Learning a deep convolutional network for image super-resolution. In: Computer Vision–ECCV 2014, pp. 184–199. Springer (2014) 2, 3, 7, 8, 14
3. Dong, C., Loy, C.C., He, K., Tang, X.: Image super-resolution using deep convolutional networks. IEEE transactions on pattern analysis and machine intelligence 38(2), 295–307 (2016) 2, 3, 4
4. Freeman, W.T., Pasztor, E.C., Carmichael, O.T.: Learning low-level vision. International journal of computer vision 40(1), 25–47 (2000) 1, 3
5. He, K., Zhang, X., Ren, S., Sun, J.: Deep residual learning for image recognition. arXiv preprint arXiv:1512.03385 (2015) 2, 4, 5, 7
6. He, K., Zhang, X., Ren, S., Sun, J.: Identity mappings in deep residual networks. arXiv preprint arXiv:1603.05027 (2016) 2, 4, 5, 6, 7
7. Huang, J.B., Singh, A., Ahuja, N.: Single image super-resolution from transformed self-exemplars. In: 2015 IEEE Conference on Computer Vision and Pattern Recognition (CVPR). pp. 5197–5206. IEEE (2015) 7, 8
8. Irani, M., Peleg, S.: Motion analysis for image enhancement: Resolution, occlusion, and transparency. Journal of Visual Communication and Image Representation 4(4), 324–335 (1993) 1
9. Kim, J., Lee, J.K., Lee, K.M.: Accurate image super-resolution using very deep convolutional networks. In: Proceedings of the IEEE Conference on Computer Vision and Pattern Recognition (2016) 2, 4, 6, 7, 8, 14
10. Krizhevsky, A., Sutskever, I., Hinton, G.E.: Imagenet classification with deep convolutional neural networks. In: Advances in neural information processing systems. pp. 1097–1105 (2012) 6
11. Liang, Y., Wang, J., Zhang, S., Gong, Y.: Incorporating image degeneration modeling with multitask learning for image super-resolution. In: Image Processing (ICIP), 2015 IEEE International Conference on. pp. 2110–2114. IEEE (2015) 1
12. Liang, Y., Wang, J., Zhou, S., Gong, Y., Zheng, N.: Incorporating image priors with deep convolutional neural networks for image super-resolution. Neurocomputing (2016) 2
13. Salvador, J., Pérez-Pellitero, E.: Naive bayes super-resolution forest. In: Proceedings of the IEEE International Conference on Computer Vision. pp. 325–333 (2015) 2
14. Schulter, S., Leistner, C., Bischof, H.: Fast and accurate image upscaling with super-resolution forests. In: Proceedings of the IEEE Conference on Computer Vision and Pattern Recognition. pp. 3791–3799 (2015) 2, 8, 14
15. Simonyan, K., Zisserman, A.: Very deep convolutional networks for large-scale image recognition. arXiv preprint arXiv:1409.1556 (2014) 2
16. Timofte, R., De, V., Gool, L.V.: Anchored neighborhood regression for fast example-based super-resolution. In: Computer Vision (ICCV), 2013 IEEE International Conference on. pp. 1920–1927. IEEE (2013) 2, 7
17. Timofte, R., De Smet, V., Van Gool, L.: A+: Adjusted anchored neighborhood regression for fast super-resolution. In: Computer Vision–ACCV 2014, pp. 111–126. Springer (2014) 2, 8

18. Wang, Z., Liu, D., Yang, J., Han, W., Huang, T.: Deep networks for image super-resolution with sparse prior. In: Proceedings of the IEEE International Conference on Computer Vision. pp. 370–378 (2015) 3
19. Yang, C.Y., Ma, C., Yang, M.H.: Single-image super-resolution: A benchmark. In: Computer Vision–ECCV 2014, pp. 372–386. Springer (2014) 7
20. Yang, J., Wright, J., Huang, T., Ma, Y.: Image super-resolution as sparse representation of raw image patches. In: Computer Vision and Pattern Recognition, 2008. CVPR 2008. IEEE Conference on. pp. 1–8. IEEE (2008) 1, 7
21. Zhang, K., Wang, B., Zuo, W., Zhang, H., Zhang, L.: Joint learning of multiple regressors for single image super-resolution. IEEE Signal Processing Letters 23(1), 102–106 (2016) 1
22. Zhang, K., Zhou, X., Zhang, H., Zuo, W.: Revisiting single image super-resolution under internet environment: Blur kernels and reconstruction algorithms. In: Pacific Rim Conference on Multimedia. pp. 677–687. Springer (2015) 1

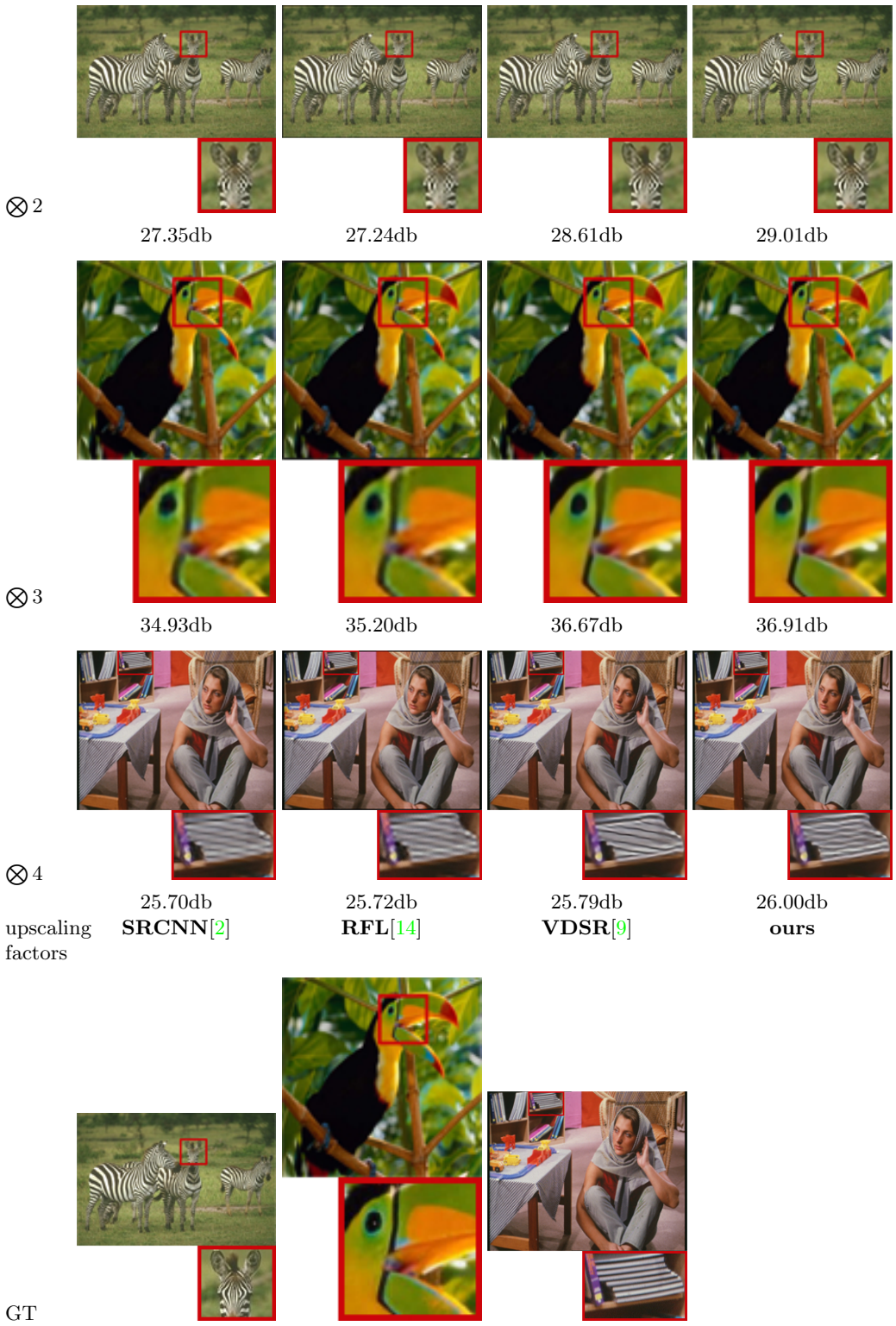

Fig. 5. Comparisons of image SR results with different methods of different upscaling factors